Ekman Heat Transport for Slab Oceans

Francis Codron

Abstract A series of schemes designed to include various representation of the Ekman-driven heat fluxes in slab-ocean models is introduced. They work by computing an Ekman mass flux, then deducing heat fluxes by the surface flow and an opposite deep return flow. The schemes differ by the computation of the return flow temperature: either diagnosed from the SST or given by an active second layer. Both schemes conserve energy, and use as few parameters as possible.

Simulations in an aquaplanet setting show that the schemes reproduce well the structure of the meridional heat transport by the ocean. Compared to a diffusive slab-ocean, the simulated SST is more flat in the tropics, and presents a relative minimum at the equator, shifting the ITCZ into the summer hemisphere. In a realistic setting with continents, the slab model simulates correctly the mean state in many regions, especially in the Tropics. The lack of other dynamical features such as barotropic gyres, means that an optimal mean-state in regions such as the mid-latitudes will require additional flux corrections.

1 Introduction

The slab ocean model, in which the ocean is represented as a single fixed-depth layer with a homogeneous temperature, is the simplest ocean model for studies of ocean-atmosphere interactions after the swamp ocean (Meehl, 1992). Even now that computational constaints are less restrictive, it still has a number of important uses.

F. Codron
Laboratoire de Météorologie Dynamique, Université Pierre et Marie Curie-Paris 6 / CNRS
Tel.: +33-1-44277352
Fax: +33-1-44276272
E-mail: fcodron@lmd.jussieu.fr

The first one is to provide a simple model for mechanistic studies, that retains the physics of ocean-atmosphere coupling through surface heat fluxes, and is very easy to interpret. Exemples of studies in realistic settings include Blade (1997) or Lau and Nath (1996). The slab ocean is also useful in idealised geometries such as aquaplanets, where it is a simple energy-conserving model of the surface. This framework can be used to study moist atmospheric dynamics (Frierson et al, 2006) or to compare atmospheric physics as proposed with fixed SSTs by Neale and Hoskins (2000). Experiments with climate models requiring very long integrations or multiple simulations with varying coefficients, that are common for exemple in paleoclimate studies because of the many unknown parameters, may also require the use of a slab ocean because the spin-up time of a full ocean GCM would be too time consuming (e.g. Donnadieu et al (2006)).

As the temperature of a slab ocean is forced only by local surface heat fluxes, it will be very different from the observed one without some representation of the heat transport by ocean currents. The most usual way to achieve this is to add a seasonal forcing equal to the surface fluxes from an atmospheric simulation forced by observed SSTs (with possible iterations), the idea being that there is an approximate balance in the surface mixed layer at this timescale between the surface fluxes and the effect of ocean dynamics. This process allows to obtain realistic SSTs for the present climate, but becomes less satisfactory for different climates as the hypothesis of an oceanic heat transport equal to the present one becomes less realistic. When the geometry of continents changes, for idealised settings or remote paleoclimates, this solution becomes impossible to use.

An alternative way of simulating the heat transport is to add a horizontal diffusion of temperature (Donnadieu et al, 2006). This is however not a very good way of representing heat transport in the ocean, as the meridional heat flux is

largest in the tropics where the meridional temperature gradient is almost flat (Trenberth and Caron, 2001). A diffusion coefficient varying with latitude can help (DeConto and Pollard, 2003) but still does not have the right dynamics and is for example unable to simulate the relative minimum of the surface temperature at the equator.

Observations (Levitus, 1987) show that the the largest contributor to the meridional heat transport in the ocean in the tropics (where the transport is strongest) is the Ekman-driven transport. This transport is organised in mean meridional cells, with a wind-driven Ekman flow in the surface mixed layer, and a return flow at depth (Schott et al, 2004). The associated vertically-integrated heat transport can be understood as the product of the mass flux multiplied by the temperature difference between the surface and return flows (Held, 2001; Czaja and Marshall, 2006). In aquaplanet settings, the meridional heat transport by the ocean as simulated by full GCMs (Marshall et al, 2007; Smith et al, 2006) is dominated by eddy diffusivity and, especially in the tropics, Ekman transport. In the presence of meridional barriers (such as continents), other heat transport components such as horizontal gyres or the overturning circulation can make a smaller global contribution (Jayne and Marotzke, 2001; Enderton and Marshall, 2009) that can even be dominant in some regions.

Anomalies of the surface branch of the Ekman heat transport have been included in studies of the role and origin of mid-latitude SST anomalies using a slab-ocean model (Alexander and Scott, 2008; Peng et al, 2006), and their role was shown to be significant. The method however only included the Ekman heat fluxes in the surface layer far from the continents and the equator (where upwelling would be strong). It also used only anomalies and not the total transport.

The aim of this paper is to introduce and test a class of schemes to represent the complete Ekman heat transport in a slab ocean context, which can thus be used in conjunction with a parameterisation of eddy diffusion to approximate the heat transport by ocean currents. The main goals are to reproduce the structure of the Ekman-driven meridional heat transport, as well as the general structure of tropical SSTs with colder waters due to upwelling at the equator and continental boundaries. The constraints will be that the scheme is energy-conserving and keeps low numerical costs and complexity, consistent with the slab model.

The rationale and implementation of two different schemes are presented in section 2. The impact of the schemes is then tested, first in an aquaplanet setting (section 3) then in a simulation of the present Earth (section 4). We then discuss the merits of the proposed schemes and conclude.

2 Description

2.1 General Principle

The momentum balance for large-scale horizontal motions in the oceanic surface mixed layer is derived starting from the primitive equations. In the small Rossby number approximation, the relative acceleration term involving large-scale velocities, as well as the spherical terms, can be neglected. The turbulent momentum fluxes remain as they are important in the mixed layer. The resulting equations are:

$$\begin{cases} \varepsilon u - fv = & -1/\rho_0 \partial_x P + \partial_z(\overline{u'w'}) \\ \varepsilon v + fu = & -1/\rho_0 \partial_y P + \partial_z(\overline{v'w'}) \end{cases} \quad (1)$$

The last term of each equation is the vertical divergence of turbulent momentum fluxes, and ε represents the various dissipative effects (including horizontal momentum fluxes), here modeled as Rayleigh linear drag. In the absence of pressure gradients, the flow is driven by the surface stresses (τ_x, τ_y). The resulting total mass transport can then be obtained by integrating equation (1) multiplied by ρ_0 from the surface, where the turbulent eddy fluxes are equal to $1/\rho_0 (\tau_x, \tau_y)$, to a depth below the surface mixed layer where they vanish:

$$\begin{cases} \varepsilon M_x - f M_y = & \tau_x \\ \varepsilon M_y + f M_x = & \tau_y \end{cases} \quad (2)$$

Note that the ocean was considered as homogeneous in this calculation (ρ_0 is constant). The zonal and meridional components of the mass transport M_x, M_y are then given by

$$\begin{cases} M_x = & (\varepsilon \tau_x + f \tau_y)/(\varepsilon^2 + f^2) \\ M_y = & (\varepsilon \tau_y - f \tau_x)/(\varepsilon^2 + f^2) \end{cases} \quad (3)$$

If ε is small compared to the Coriolis factor f, the classic Ekman drift formula is recovered. The presence of ε allows the computation of the mass transport even at the equator where f vanishes and the Ekman drift becomes singular.

The Ekman transport schemes will use these mass fluxes to compute the total heat fluxes. The net vertically-integrated heat flux across some horizontal boundary will be given by the sum of the heat transports by the Ekman flow at the temperature of the surface mixed-layer (i.e. the slab temperature), and by a deep return flow that is assumed to have exactly the opposite mass flux but takes place at a lower temperature. The schemes will essentially differ in how the temperature of the return flow and its influence on the slab temperature are computed.
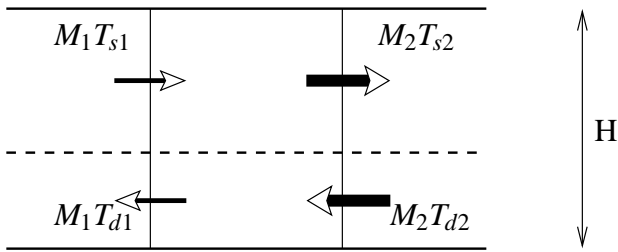
Fig. 1 Heat fluxes in the 1.5-layer scheme. Both Ekman and return flow occur in the unique slab layer of depth H, but at different temperatures. The mass fluxes $M_{1,2}$ are computed from the wind stress, and the temperatures at the interfaces $T_{1,2}$ from the slab temperature at the grid-points.

Fig. 2 Heat fluxes in the 2-layers scheme. The Ekman and return flow are opposite and occur in two distinct slab layers. The vertical mass flux is obtained by continuity.

2.2 1.5 Layer model

The first implementation is schematized on figure 1 along one horizontal dimension. Only one prognostic temperature for the surface (slab) layer T_s is used. The temperature at depth T_d, that will be used for the deep return flow, is then diagnosed from T_s:

$$T_d = \alpha T_s + (1 - \alpha) T_0 \qquad (4)$$

Where T_0 is the freezing temperature of seawater. This formulation ensures that T_d remains above freezing and below the surface temperature T_s. The difference between T_s and T_d will be largest in the Tropics, which is consistent with the temperature of the ocean being more horizontally uniform at depth than at the surface. Choosing a value of $\alpha = 2/3$ gives a temperature of the return flow, or of the upwelled water, about 10°cooler than the surface one in the tropics, which seems reasonable.

The evolution of the slab temperature at a given grid point is then given by the convergence of the total (surface plus deep) heat flux through the boundaries:

$$\rho H S \frac{\partial T_s}{\partial t} = M_1 (T_{s1} - T_{d1}) - M_2 (T_{s2} - T_{d2}) \qquad (5)$$

Using figure 1 notations, with S the area of the grid point. The temperatures at the interfaces T_1, T_2 can be estimated from T_s and T_d at neighbouring grid points using any advection scheme: upstream, centered or more complex ones. The heat transport scheme will conserve energy as long as the same interface temperature is used for the evolution of the temperatures of the grid points on both sides.

With $T_s > T_d$, the net heat flux through a grid boundary has the sign of the surface Ekman mass flux. There is thus a poleward heat transport under the trade winds, which becomes equatorwards in regions of surface westerlies. A divergent Ekman mass flux will lead to a local cooling, reproducing the effect of the upwelling of deep water even though there is no explicit upwelling in this scheme.
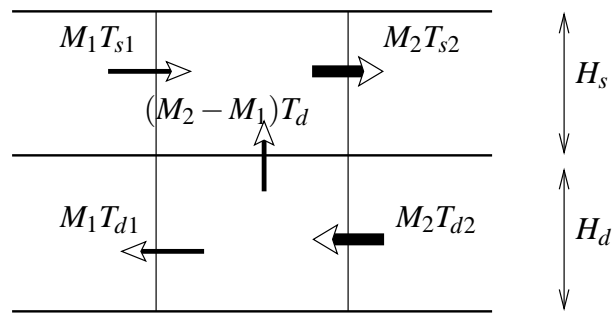
In the case of a convergent Ekman mass flux, the slab temperature will warm, which is not so realistic: there would in reality be a sinking of the surface water and a deepening of the thermocline, as observed in the subtropics, instead of a warming of the surface layer. This spurious warming is a weakness of this 1.5 layer scheme, but it can be mitigated using a variable coefficient α. For that purpose, values of the net mass flux $(M_1 - M_2)$ and of the total flux exchanged $(|M_1| + |M_2|)$ through the boundaries of a grid point are computed. The value of α then varies according to the ratio between the net and total values. It is equal to 1/3 when the ratio approaches -1 (purely divergent flux with M_1 and M_2 of opposite signs) and to 1 with a ratio of 1 (purely convergent flux). In the latter case, the deep temperature becomes equal to the surface one, and the net heat flux through a boundary cancels out.

2.3 2-Layers model

As its name suggests, the 2-layers model uses two surface and deep slab layers with prognostic temperatures. The deep layer is generally taken with a larger thickness, typically between 150 and 350m. All the surface heat fluxes are exchanged with the surface layer. The horizontal temperature advection is computed as in the 1.5-layer case, but using the Ekman mass fluxes in the surface layer, and the opposite return fluxes in the bottom layer (figure 2). In addition, there is an upwelling or downwelling mass flux between the surface and deep layers, which is equal to the divergence of the horizontal Ekman mass flux. The resulting vertical heat flux is computed using an upstream scheme, to ensure no convergence of heat in the surface layer in the case of a convergent mass flux (downwelling). Finally, we use a simple convective adjustment to ensure that the deep temperature remains lower then the surface one. It is active in the winter mid- and high-latitudes.

2.4 Implementation

The slab ocean is used as the surface model coupled to the LMDZ atmospheric GCM (Hourdin et al, 2006), a model using finite-difference schemes on a regular latitude-longitude grid. The simulations use a relatively low resolution of 48x48 grid points on the horizontal, or 7.5 degrees in longitude by 3.75 in latitude. This allows to do extensive testing , and is consistent with potential uses of the slab ocean for long simulations. We performed some tests where the resolution has been uniformly doubled to 96 by 96 points, but the results were very similar apart from the impact of the resolution on the atmospheric mean-state. Both configurations use 19 sigma-levels on the vertical. The timestep used is 6 mn for the atmospheric dynamics, and 30 mn for the physical parameterisations (including the slab ocean). Over land, the ORCHIDEE land surface model is used (Krinner et al, 2005).

The slab ocean shares the horizontal grid of the atmospheric GCM. A simple one-layer thermodynamic sea-ice model is added, whose complexity is comparable to the ocean model; it is described in more details in the appendix. The ocean temperatures at the interfaces are computed using an upstream advection scheme, except in the meridional direction for the 2-layers version where a centered scheme is used. With the upstream scheme, the temperature of the advected deep water could become higher than the surface one in the case of a strong surface temperature gradient and a weak vertical gradient, as happens in the winter mid-latitudes. When continents are present, the mass flux - and thus heat flux - is set to zero at ocean-continent boundaries.

In addition to the heat transport by Ekman currents, horizontal temperature diffusion is used in the ocean with a constant diffusivity coefficient. We use a coefficient of $25000\,\mathrm{m^2.s^{-1}}$ for a single 50m-deep slab layer. This value was chosen so that the diffusive meridional heat transport would peak above 1 PW in the aquaplanet setting, similar to the one simulated by full GCMs (Marshall et al, 2007). The diffusivity coefficient is thus large, as all the heat transport takes place in the 50-m surface layer. When the depths of the oceanic layers change, the diffusion coefficient varies in inverse proportion to the total depth. The vertically-integrated heat transport thus remains approximately the same with different total depths or formulations (1.5 or 2 layers), provided that the horizontal temperature gradient does not vary too much.

The complete equation of evolution of the temperature of the slab ocean T_s is then, for the 1.5-layer case:

$$\frac{\partial T_s}{\partial_t} = \frac{1}{\rho C H} \left(F_{a-o} + F_{i-o}\right) - D\Delta T_s - \frac{1}{\rho H} \mathrm{div}_H \left[\mathbf{M}\left(T_s - T_d\right)\right]$$
(6)
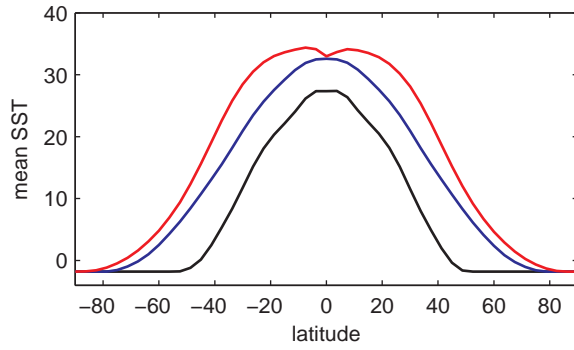
Fig. 3 Annual and zonal-mean Slab-ocean temperature, for no heat transport (black), diffusive transport (blue), and diffusive plus 1.5 layer Ekman transport (red)

Where F_{a-o} and F_{i-o} are the heat fluxes from the atmosphere and the sea ice, respectively, D is the horizontal diffusion coefficient, and div_H is the horizontal divergence operator. The values of the Ekman mass flux $\mathbf{M}$ (from equation 3), and of the surface and deep temperatures T_s and T_d used to compute the divergence are evaluated on the grid-point interfaces.

In the case of the 2-layer model, the evolution equation for the surface layer becomes:

$$\frac{\partial T_s}{\partial_t} = \frac{1}{\rho C H_S} \left(F_{a-o} + F_{i-o} + F_c\right) - D\Delta T_s - \frac{1}{\rho H} \left[\mathrm{div}_H \left(\mathbf{M} T_s\right) - W T_{s/d}\right]$$
(7)

Where a new convective heat flux component F_c between the two slab layers was added. The vertical mass flux W, in $\mathrm{kg.m^{-2}.s^{-1}}$, is defined as $W = 1/H \, \mathrm{div}_H \mathbf{M}$. The vertically-advected temperature is T_s or T_d depending on the sign of W. The evolution of the deep temperature T_d is similar, only without the surface fluxes.

3 Aquaplanet results

We first test the schemes in the idealised setup of an ocean-covered planet. In the absence of meridional continental boundaries, the heat transport will be accomplished by Ekman currents and eddy diffusion. To check the impact of different representations of the heat transport, we use a series of experiments with an inert ocean (no transport), a purely diffusive transport, and finally both diffusive and Ekman transports. Starting from an idealised SST distribution, the model reaches a steady state in about 20 years.

3.1 Mean meridional structure

The zonal-mean ocean temperature for the three experiments is shown on figure 3. The associated integrated meridional heat transports are given on figure 4. In the inert ocean case, the slab temperature has a sharp peak at the equator, then drops regularly towards the ice-edge at about 50°latitude. When diffusion is added, the temperature rises by 5 to 10 degrees, but the general shape remains similar. The poleward heat transport, peaking around 1PW in the mid-latitudes (figure 4, top), causes a reduction of the sea-ice extent. The effect on the albedo, added to other feedbacks such as increased water vapor, explains the general warming observed.

The structure of the SST and meridional transport change when the 1.5-layer Ekman transport is added. The Ekman transport is strongest in the tropics, where it peaks slightly under 3PW (figure 4, middle), because of the large temperature difference between the surface and the return flow (Czaja and Marshall, 2006). It then changes sign to become equatorward under the westerly-wind belt of the mid-latitudes. The strongly divergent heat transport at the equator leads to a local SST minimum there and to a much flatter meridional structure in the tropics (figure 3).

The structure of the SST and total heat transport ressemble the observed ones (Trenberth and Caron, 2001), with a maximum in the tropics decreasing to a lower transport in the mid-latitudes. The amplitude also agrees well with aquaplanet results using full ocean GCMs (Marshall et al, 2007; Smith et al, 2006). Going into details, the diffusive transport is directed equatorward only very close to the equator in our results, compared to throughout the tropics (and with a larger magnitude) in the GCMs. This is a consequence of the deep thermocline in the subtropics, that is not represented in a slab ocean. This error is compensated by a weaker Ekman transport in the tropics for the slab model.

The temperature of the two slab-layers for the 2-layers model is shown on figure 5. The surface layer has an intermediate structure between the diffusive and 1.5-layer models: the equatorial minimum is present and the tropical temperature is flattened, but not as much as with 1.5 layers. The reason is a reduced magnitude of the tropical Ekman heat transport (figure 4) due to a smaller temperature difference with the subsurface. Figure 5 indeed shows that the deep layer temperature is only about 5 degrees cooler than the surface.
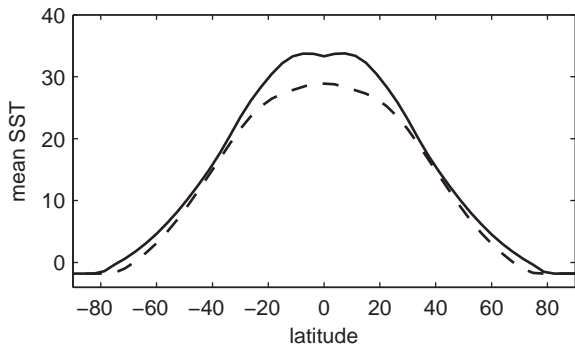
3.2 Seasonal cycle

The seasonal cycles of the SST and precipitation for the diffusive slab ocean are shown on figure 6. The maxima of SST and the ITCZ wander a short distance around the equator, following the sun's movement with a few months delay.
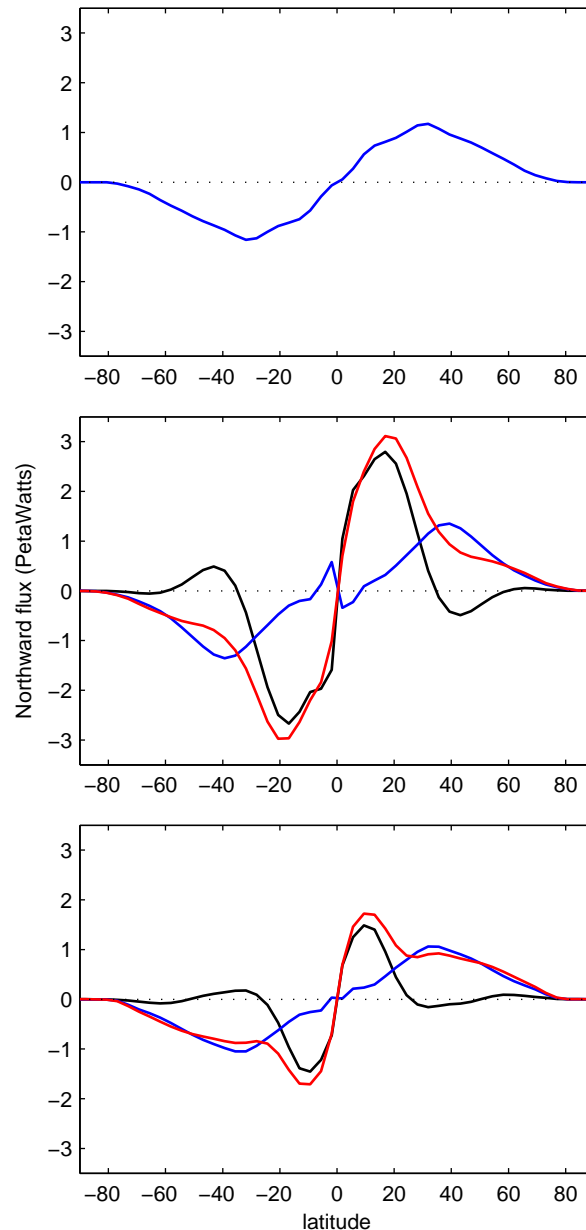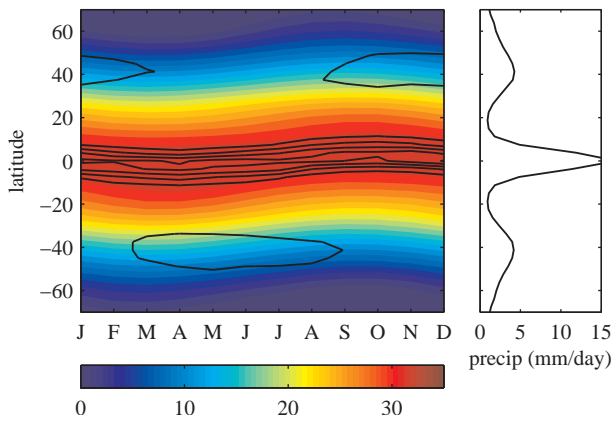

Fig. 4 Oceanic meridional heat transport (in PW): diffusive (blue), Ekman (black) and total (red). Simulations with (top) diffusion only, (middle) 1.5-layer Ekman, (bottom) 2-layer Ekman.

The annual-mean precipitation has a sharp maximum on the equator.

When Ekman transport is added (1.5-layer, figure 7), the equatorial upwelling prevents precipitation there. The ITCZ instead jumps from one hemisphere to another between seasons, and the annual-mean shows two distinct maxima on both sides of the equator. There is in this simulation a strong meridional coupling between the SST, meridional wind and ITCZ in the vicinity of the equator: with a non-zero ε coefficient, mass fluxes are in the direction of the wind stress close to the equator. When the warm SSTs and the ITCZ

Fig. 5 Annual and zonal-mean Slab-ocean temperature, with the 2-layers Ekman transport. Surface layer (cont) and bottom layer (dashed).

Fig. 7 Same as figure 6 for the 1.5-layer experiment.

Fig. 6 Diffusive ocean experiment: left, seasonal cycle of the ocean temperature (colour) and precipitation (contours every 4 mm/day). Right, annual-mean precipitation.
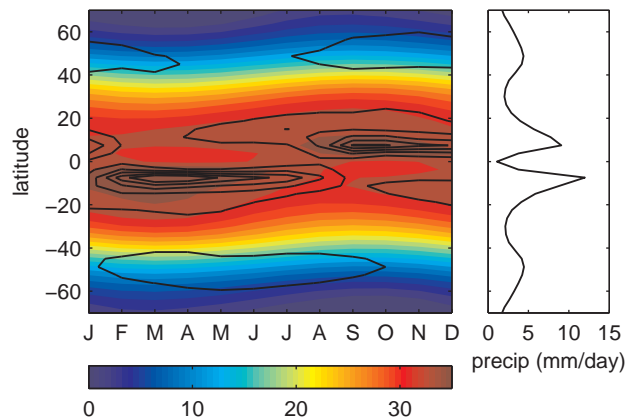
are in the north, the southerly cross-equatorial winds then induce an upwelling to the south and a downwelling to the north, reinforcing the SST gradients and the ITCZ position.

The position of the mid-latitude storm tracks, as indicated by secondary precipitation extrema, are located farther poleward in the simulation with Ekman transport. This is consistent with a tropical SST distribution more flat and extended in latitude.

The results with the 2-layers Ekman transport are similar to the 1.5-layer ones, except that the meridional SST gradients are less strong. The precipitation structure retains its double peak.

4 Present Climate

We now test the impact of the Ekman transport schemes in the actual Earth configuration, using present-day insolation and greenhouse gas concentrations. A land-surface and vegetation scheme is used over the continents. No flux correc-

tion is applied in the ocean, so the slab temperature is driven only by the surface heat fluxes and the parameterised Ekman and diffusive heat transports. Starting from an idealised zonal-mean SST, the simulated mean state converges in ten to thirty years.

The annual-mean temperature of the surface slab layer is shown on figure 8 for the different heat transport schemes, together with the areas of minimal and maximal seasonal sea-ice extent. As in the aquaplanet experiments, both simulations including a representation of the Ekman transport are globally warmer, and have a tropical belt of warm SSTs with a more flat latitudinal shape. In addition, there is a marked cooling by the upwelling at the eastern ocean boundaries and in the central Pacific, that is more pronounced in the 1.5-layer simulation. There is also a hint of a spurious upwelling-induced cooling in the eastern Indian Ocean.

The minimum sea-ice extent is similar in the three cases: thick sea ice occupies the Arctic Ocean year-round because of the lack of drift and export out of the Arctic in the model; in the Antarctic almost all the ice melts in summer. The maximum extent is too large with diffusion only; it is better estimated with the addition of Ekman transport. The 1.5-layer model has a larger maximum extent in both hemispheres than the 2-layer model, possibly due to the larger amplitude of the seasonal cycle in the mid-latitudes, as discussed later on. The ice extent is in any case strongly dependent on parameters of the model such as the snow and ice albedos.
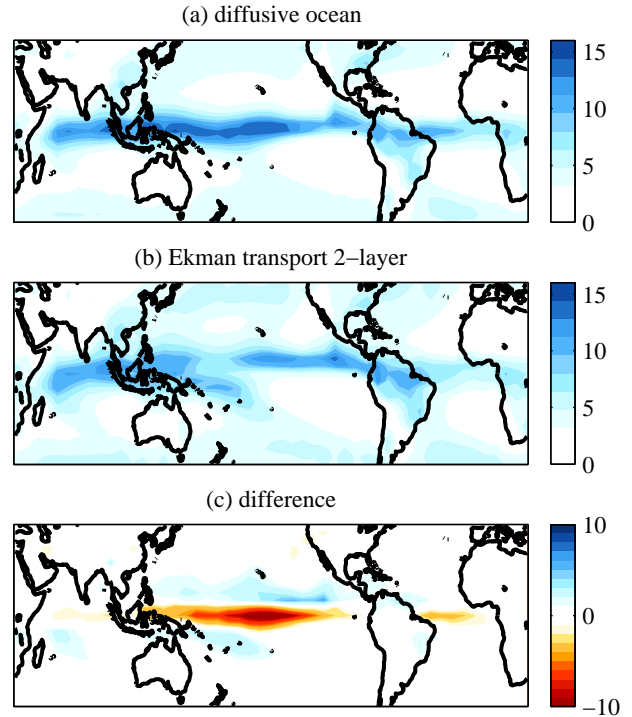
The changes in the mean tropical precipitation brought by the inclusion of Ekman transport are shown on figure 9. For the diffusive ocean, the precipitation belt is centered on the equator. When the 2-layer Ekman transport is added, precipitation amounts decrease strongly at the equator and increase on both sides, giving a structure much closer to the observed one. In particular, the eastern-Pacific ITCZ remains to the north of the equator. There is a also a small increase in monsoonal rains over East Asia and South Amer-

(a) diffusive ocean

(b) Ekman transport 1.5–layer

(c) Ekman transport 2–layer
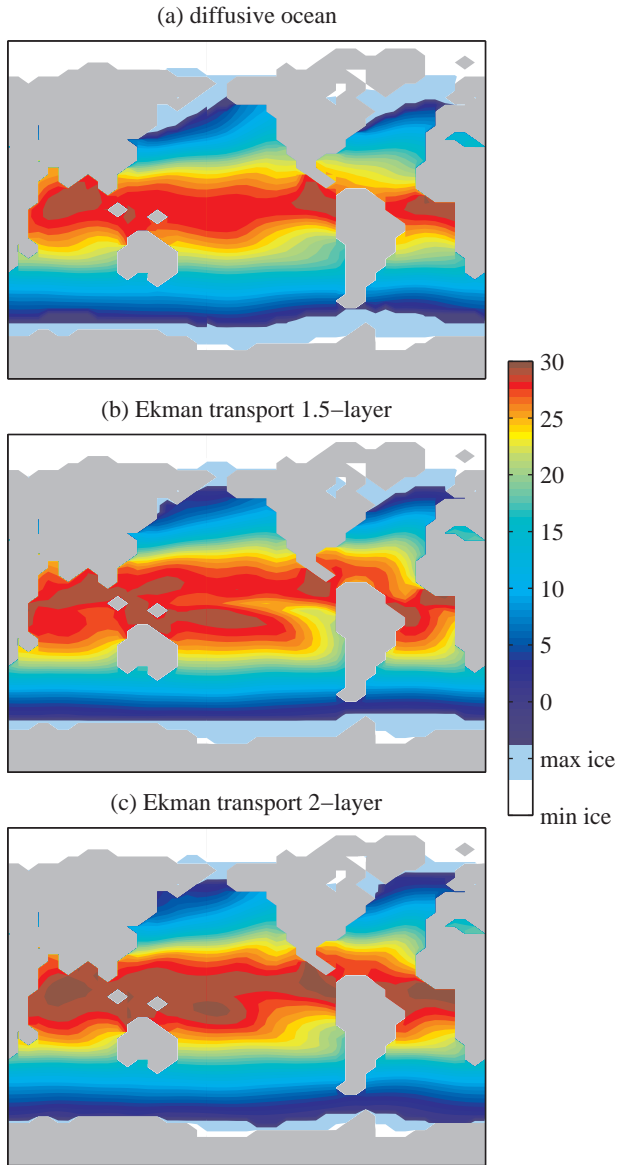
Fig. 8 Annual-mean SST in °C (colors), and minimum (white) and maximum (light blue) seasonal sea-ice extent, for different simulations of the present climate: (a) diffusive slab ocean, and additional (b) 1.5-layer (c) 2-layer Ekman transport.

(a) diffusive ocean

(b) Ekman transport 2–layer

(c) difference

Fig. 9 Annual-mean precipitation (mm/day) for simulations of the present climate: (a) diffusive ocean, (b) 2-layer Ekman transport, (c) the (b)-(a) difference.

ica. Using the 1.5-layer Ekman scheme brings similar changes, only stronger. In particular, the dry equatorial band in the Pacific extends all the way to the west. The model with the 1.5-layer scheme also tends to simulate unrealistically strong precipitation above some hot points where there is a convergence of surface Ekman currents.
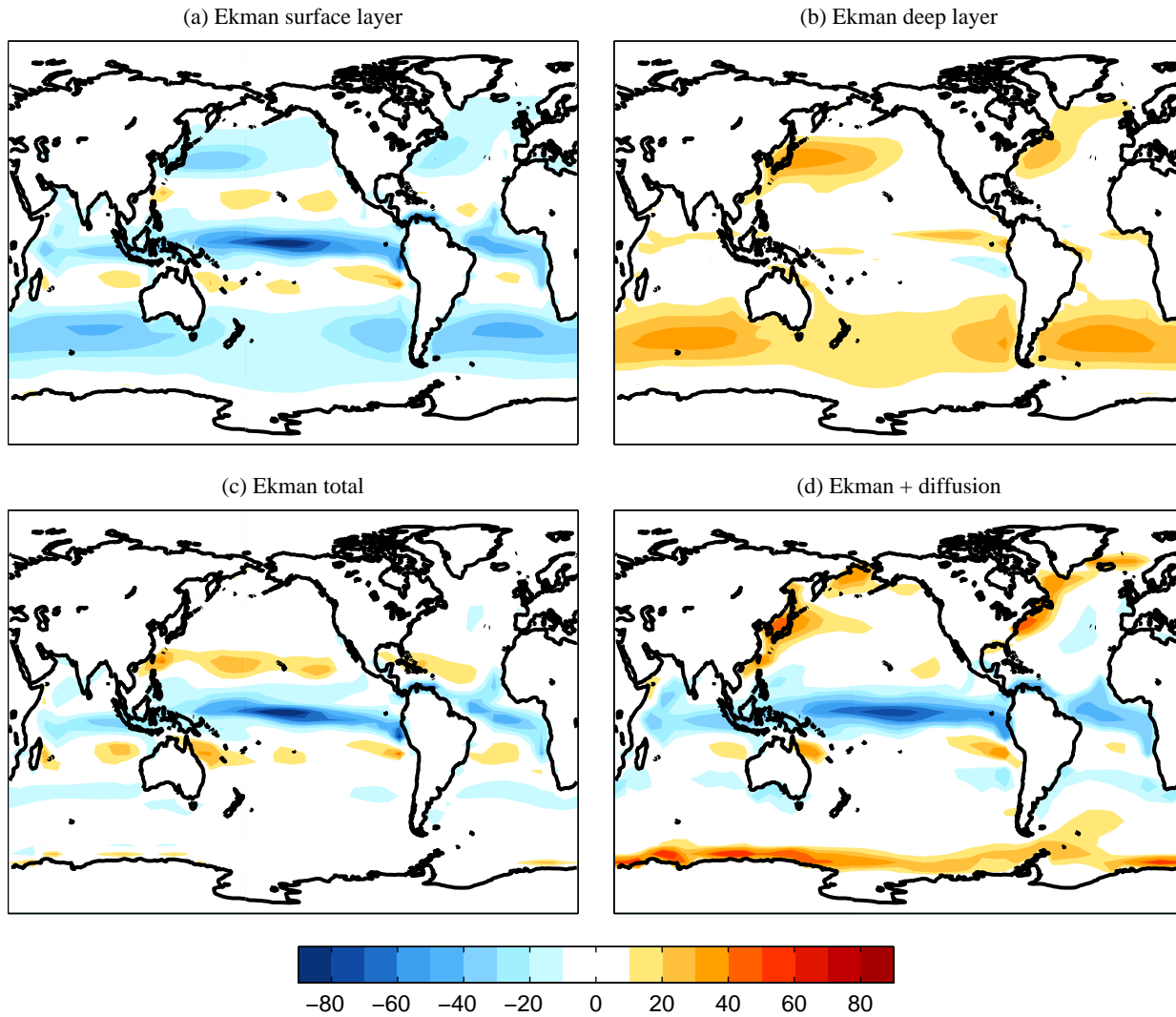
In order to better understand what the Ekman transport scheme accomplishes, figure 10 shows maps of the heating of the slab layers due to the divergence of heat fluxes, in the 2-layer case. The heating is shown in W.m^{-2} for easier comparison with the typical magnitude of surface heat fluxes.

The largest effect in the surface layer (figure 10a) is the cooling around the equator, especially in the Pacific and at eastern boundaries, where the surface Ekman currents are divergent. The cooling comes here from the upwelling of cold deep water compensating the surface divergence. At depth (figure 10b), the flat horizontal temperature structure means there is only a small warming at the equator (an upstream advection scheme is used on the vertical).

In addition to forcing in the tropics, there is a slight surface warming in the subtropics, and another belt of surface cooling in the mid-latitudes, under the westerlies. It is due not to upwelling, but to equatorwards advection of cold water. This surface advective cooling is largely compensated on average by the poleward return flow in the deeper layer, as can be seen on the vertically-integrated heating (figure 10c). There is however a significant impact on the seasonal cycle of SST (not shown): in summer, the Ekman flow cools the surface layer and warms the deeper layer; the heat stored at depth is then restored to the surface in winter through the vertical convective adjustment. Compared to the 1.5-layer scheme, in which the compensation between surface and return flows is instantaneous, the SST is then colder in fall and warmer in spring. The surface cooling or warming induced by changes in Ekman transport can also be a factor in the low-frequency variability of the mid-latitudes.

(a) Ekman surface layer

(b) Ekman deep layer

(c) Ekman total

(d) Ekman + diffusion

−80 −60 −40 −20 0 20 40 60 80

Fig. 10 Annual-mean heating of the slab ocean by the parameterised horizontal heat transports in the 2-layer model, units in W.m^{-2}. Ekman transport in (a) the surface layer, (b) the deep layer, and (c) vertically integrated; (d) sum of the integrated Ekman and diffusive transports.

The impact of the diffusive transport is apparent by comparing figures 10c and 10d, which show the total heating by the ocean currents. The horizontal diffusion is cooling the whole tropics, cancelling the Ekman-induced warming in the subtropics. The heating in mid and high latitudes is particularly strong in two areas. The first one, particularly apparent in the Southern Hemisphere, is the sea-ice edge, because of the null temperature gradient under the ice. The second one is close to the east coasts of continents in the northern hemisphere. There are no boundary currents in this model, but the SST is strongly cooled in winter through surface heat fluxes forced by the cold air blowing off the continent, and this is partially compensated by the horizontal diffusion.

5 Discussion

5.1 Role of epsilon

The schemes presented rely on only a few parameters, so that they can be used in a variety of settings. The value of ε, the inverse damping timescale of oceanic currents, turned out to have the most influence. Far from the equator, ε is small compared to the Coriolis factor f and its exact value does not matter. Closer to the equator, the surface currents become aligned with the wind stress. The transition latitude, where $\varepsilon = f$, is at 4° for $\varepsilon = 10^{-5}$ s^{-1} (used in the simulations throughout the paper), and at 2° for $\varepsilon = 5.10^{-6}$ s^{-1}. The latter value means that the equatorial region where the Coriolis force is weak is less wide than the model's resolution. It leads to strongly divergent Ekman currents and an

intense, narrow upwelling centered on the equator. With the higher value of ε, the equatorial upwelling is broader and less intense. The total upwelled flux should not change: the integrated vertical mass flux between, for example, 10°S and 10°N must compensate the poleward mass fluxes at these latitudes, which are proportional to the zonal wind stress at 10°S and 10°N but do not depend on ε. Given that the deep slab temperature is almost flat around the equator, the total cooling of the surface layer is also nearly constant.

Even though the meridional heat transport away from the equator is not much affected, the structure of the upwelling has large impacts on the tropical SST and precipitation. With the higher value of ε, a meridional current is forced at the equator by cross-equatorial winds. This causes an additional upwelling on the upwind side of the equator, and downwelling on the downwind side. The cold tongue of SST thus tends to be centered off the equator (as in the Eastern Pacific in figure 8). The meridional coupling between the SST, wind and upwelling is also strong and tends to keep the ITCZ on one side of the equator. For the lower values of ε, the coldest SSTs remain centered on the equator, and there is a tendency for meridionally-symmetric climate, with a zonally-extended cold tongue and a double ITCZ.

5.2 Comparison of the schemes

We have tested two different versions of an Ekman heat transport scheme. In the 1.5-layer scheme, the temperature of the return flow is diagnosed from the surface one. This scheme does a very good job of reproducing the mean meridional heat transport, but misses some physics associated with the independent evolutions of the surface and deep temperature. In addition, this scheme can create some spurious surface hot spots where there is a convergence of surface currents (as can happen close to continents), a problem that can be partially remedied using a variable α coefficient (section 2).

The 2-layer scheme brings a bit more complexity, with a second interactive layer and convective adjusment but has more transparent physics. Its main weakness might be an underestimation of the equatorial cooling through upwelling and of the meridional heat flux in the tropics, because the temperature of the deep water is too warm in the tropics.

Part of the problem may come from the atmospheric model: it is known to produce westerlies too close to the equator, and a temperature gradient too steep between the subtropics and midlatitudes, especially at lower resolutions (Marti et al, 2010). The global heat balance in the lower ocean layer requires that the temperature of the upwelled water is given by the temperature of the water sinking in the subtropics, minus cooling through the convective adjustment at higher latitudes. The biases of the simulated atmosphere mean that the sinking will happen too close to the equator, thus with warmer water. The lack of any representation of the role of salinity in the ocean model could also lead to an underestimation of convective exchanges in the high-latitudes and of the cooling of the deep layer.

Finally, there is a constraint coming from the model formulation. In the real ocean, the temperature below the surface mixed layer is warmer in the subtropics than closer to the equator, due to a much deeper thermocline. The 2-layer model cannot however sustain a local temperature minimum at depth at the equator, because both heat transport mechanisms (diffusion and Ekman) would then act to reduce it. A more complex vertical structure of the model would be necessary to represent these variations of the thermocline detph.

In the mid-latitudes, the impact of Ekman transport comes more from advection of the mean temperature gradient and less from the convergence or divergence of the currents. For example, increased westerlies normally have a short-term cooling impact on the SST through the induced equatorward mass transport at the surface. In the 1.5-layer scheme, this is balanced instantaneously by a return flow at a close temperature (in the mid-latitudes). In the 2-layer scheme, the temperature evolves independently in the two layers until they are connected by the convective adjustment. Inspection of the temperature tendency due to the horizontal Ekman heat transport in the different simulations indeed shows that while the variance of the vertically-integrated tendency in the mid-latitudes is larger in the 1.5-layer case (because of a larger surface-deep temperature difference), the variance in the surface layer alone is much larger with the 2-layer scheme. The 2-layer scheme thus seems more able to simulate the impact of anomalous Ekman transports on mid-latitude SST variability, although an anomaly-based scheme might be even more appropriate in that case (see below).

5.3 Improvements using observed climatologies

The heat transport schemes presented use only a small number of constant parameters, so that they can be directly used in any setting. To obtain a more realistic simulation of the present-day climate, a number of improvements could be made using climatologies derived from the observations. A first possibility is the use of prescribed instead of simulated sea-ice extent. The depth of the slab layer could also be taken to vary spatially according to observed seasonal mixed-layer depths, instead of being a uniform 50-m. The impact of the horizontal heat transport (and of surface heat fluxes) would be larger in regions of shallow surface mixed layer, such as the eastern Pacific, and lower in regions of deeper mixed layer such as the Indian Ocean, thereby increasing the SST signature of upwelling in the former and reducing it in the latter.

A more radical correction would be to add heat flux corrections to bring the seasonal simulated SST in line with the

observed one, as is classically done in inert slab ocean models. The flux corrections can then replace the missing dynamics, including the horizontal diffusion, and only the Ekman heat flux variability or sensitivity is retained. For studies restricted to the mid-latitudes, some authors (Alexander and Scott, 2008; Peng et al, 2006) developed an anomaly-based Ekman scheme in their slab ocean, in which only anomalous Ekman heat fluxes in the surface layer are added to the SST evolution equation together with the required corrections. This has the advantage of eliminating the compensation by the return flow (1.5-layer scheme) or the convective mixing with the deep layer (2-layer), and thus can work better for this specific use. Anomaly-based schemes are however unable to represent anomalous upwelling motions that are important in the Tropics or near continent boundaries.

These various improvements all rely on existing climatologies of the simulated climate, whether of sea-ice, SST, or mixed-layer depth. They can thus be used only for mechanistic studies or for sensitivity tests with small anomaly amplitudes. For climates very different from the present, such as in the distant past or with idealised - or no - continents, there is no reason for climatologies derived from present observations to hold. The schemes presented and tested in this paper were thus developped to be used without them.

6 Conclusion

We have introduced in this paper two implementations of a simple numerical scheme to simulate the oceanic heat transport by the Ekman surface currents and the compensating return flow, in a slab-ocean setting covering the whole ocean. They both rely on computing a mass flux from the surface wind stress, and using it to advect heat. The difference comes from the temperature of the return flow, which can be diagnosed or given by a second interactive slab layer. The schemes conserve energy, and allow for a fast spin-up of the ocean. They have been tested together with a simple horizontal diffusion representing the action of eddies as a complete representation of heat transport by currents.

The structure of the meridional heat transport simulated in an aquaplanet setting agrees well with the one from full GCMs (Smith et al, 2006; Marshall et al, 2007), with a maximum in the tropics and a drop before the mid-latitudes. The amplitude also agrees well, especially for the 1.5-layer scheme. In comparison with diffusive-only heat transport, both schemes produce a flat SST in the tropics, with a relative annual-mean minimum at the equator. The ITCZ alternates between the hemispheres, and is coupled in the meridional direction with the meridional wind and SST gradients.

A simulation of the present-day climate with realistic continents and vegetation yields a climate that is reasonable given the resolution used. In particular, the equatorial cold tongue and eastern boundary upwelling systems are well reproduced. There are some regional problems, such as a tendency for upwelling in the Indian ocean and a Gulf of Guinea that is too warm; but most of the main biases are also present in simulations with the same model coupled to a full ocean GCM.

The main limitation of the schemes (which is not an issue for aquaplanets) is the lack of heat transport by the horizontal gyres: their contribution is significant in the mid-latitudes and can further change the mean state through ice-albedo feedbacks (Enderton and Marshall, 2009). If the simulated climate needs to be the closest possible to observed, this and other weaknesses can be corrected with the usual flux correction added to slab models; the sensitivity of the ocean temperature to the surface wind through Ekman transport will be retained.

A Sea-ice model

The simple thermodynamic sea-ice model used throughout the paper was built to provide an interactive representation of the sea-ice, of a complexity comparable to the one of a slab ocean. Changes in the sea-ice model, or in parameters such as the snow albedo, can have a large impact on the simulated climate, changing the ice extent and the global temperature through the ice-albedo feedback. This effect is however largely independent of the heat transport schemes that are the focus of this paper.

A.1 Representation of the ice

Over each grid point, the sea ice is represented by a uniform layer of depth H and fractional area f. It may be covered by a layer of snow that has a zero heat capacity. The temperature at the bottom of the ice layer is always equal to the freezing temperature of sea water T_0, while the surface temperature T_s, seen by the atmosphere, can vary. The temperature profile within the ice layer is assumed to be linear, so that the mean ice temperature is $(T_s + T_0)/2$. The evolution of T_s is then given by:

$$\frac{\partial T_s}{\partial t} = \frac{2}{\rho_i C_i H} \left(F_{a-i} - F_{i-o} \right) \tag{8}$$

Where ρ_i and C_i are the volumic mass and specific heat capacity of the ice, and F_{a-i} and F_{i-o} are the heat fluxes from the atmosphere to the ice, and from the ice to the ocean. The latter is computed from the temperature gradient within the ice layer:

$$F_{i-o} = \frac{\lambda}{H} \left(T_s - T_0 \right) \tag{9}$$

with λ the conductivity of the ice.

A.2 Ice formation and melting

As soon as the temperature of the surface slab ocean layer falls below freezing, the temperature is set back to T_0, and the resulting energy difference is used to build ice mass and, if ice is already present, to bring it to the same mean temperature. A set of rules is used to determine how the new mass is divided between an extension of the fractional area and a thickening. If the ocean temperature becomes positive, ice is melted and the ocean temperature brought back to T_0 in a reverse process.

If the surface temperature of the ice T_s becomes positive, through surface heat fluxes, it is similarly brought back to freezing level, and the energy difference in the ice layer is used to first melt the snow mass, if present, then part of the ice mass. Any energy left after all the ice is melted is used to warm the ocean, ensuring energy conservation.

References

Alexander MA, Scott JD (2008) The role of ekman ocean heat transport in the northern hemisphere response to ENSO. Journal of Climate 21(21):5688–5707

Blade I (1997) The influence of midlatitude ocean-atmosphere coupling on the low-frequency variability of a gcm .1. no tropical sst forcing. J Climate 10(8):2087–2106

Czaja A, Marshall J (2006) Partitioning of poleward heat transport between the atmosphere and ocean. J Atmos Sci 63(5):1498–1511

DeConto RM, Pollard D (2003) Rapid cenozoic glaciation of antarctica induced by declining atmospheric CO2. Nature 421(6920):245–249, DOI 10.1038/nature01290

Donnadieu Y, Pierrehumbert R, Jacob R, Fluteau F (2006) Modelling the primary control of paleogeography on cretaceous climate. Earth and Planetary Science Letters 248(1-2):426–437, DOI 10.1016/j.epsl.2006.06.007

Enderton D, Marshall J (2009) Explorations of Atmosphere–Ocean–Ice climates on an aquaplanet and their meridional energy transports. Journal of the Atmospheric Sciences 66(6):1593–1611

Frierson DMW, Held IM, Zurita-Gotor P (2006) A Gray-Radiation aquaplanet moist GCM. part i: Static stability and eddy scale. Journal of the Atmospheric Sciences 63(10):2548–2566

Held IM (2001) The partitioning of the poleward energy transport between the tropical ocean and atmosphere. Journal of the Atmospheric Sciences 58(8):943–948

Hourdin F, Musat I, Bony S, Braconnot P, Codron F, Dufresne J, Fairhead L, Filiberti M, Friedlingstein P, Grandpeix J, Krinner G, LeVan P, Li Z, Lott F (2006) The LMDZ4 general circulation model: climate performance and sensitivity to parametrized physics with emphasis on tropical convection. Climate Dynamics 27(7):787–813, DOI 10.1007/s00382-006-0158-0

Jayne SR, Marotzke J (2001) The dynamics of ocean heat transport variability. Reviews of Geophysics 39(3):385–411, DOI 200110.1029/2000RG000084

Krinner G, Viovy N, de Noblet-Ducoudré N, Ogée J, Polcher J, Friedlingstein P, Ciais P, Sitch S, Prentice IC (2005) A dynamic global vegetation model for studies of the coupled atmosphere-biosphere system. Global Biogeochemical Cycles 19:33 PP., DOI 200510.1029/2003GB002199

Lau NC, Nath MJ (1996) The role of the atmospheric bridge in linking tropical pacific enso events to extratropical sst anomalies. Journal of Climate 9(9):2036–2057, DOI 10.1175/1520-0442(1996)009¡2036:TROTBI¿2.0.CO;2

Levitus S (1987) Meridional ekman heat fluxes for the world ocean and individual ocean basins. Journal of Physical Oceanography 17(9):1484–1492

Marshall J, Ferreira D, Campin JM, Enderton D (2007) Mean climate and variability of the atmosphere and ocean on an aquaplanet. JOURNAL OF THE ATMOSPHERIC SCIENCES 64(12):4270–4286

Marti O, Braconnot P, Dufresne J, Bellier J, Benshila R, Bony S, Brockmann P, Cadule P, Caubel A, Codron F, de Noblet N, Denvil S, Fairhead L, Fichefet T, Foujols M, Friedlingstein P, Goosse H, Grandpeix J, Guilyardi E, Hourdin F, Idelkadi A, Kageyama M, Krinner G, Lévy C, Madec G, Mignot J, Musat I, Swingedouw D, Talandier C (2010) Key features of the IPSL ocean atmosphere model and its sensitivity to atmospheric resolution. Climate Dynamics 34(1):1–26, DOI 10.1007/s00382-009-0640-6

Meehl GA (1992) Climate System Modeling, Cambridge University Press, chap Global coupled models: Atmosphere, ocean, sea ice, pp 555–581

Neale RB, Hoskins BJ (2000) A standard test for AGCMs including their physical parametrizations: I: the proposal. Atmospheric Science Letters 1(2):101–107, DOI 10.1006/asle.2000.0022

Peng S, Robinson WA, Li S, Alexander MA (2006) Effects of ekman transport on the NAO response to a tropical atlantic SST anomaly. Journal of Climate 19(19):4803, DOI 10.1175/JCLI3910.1

Schott FA, McCreary J, Johnson G (2004) Earth Climate: The Ocean-Atmosphere Interaction, AGU Geophysical Monograph Series, chap Shallow overturning circulations of the tropical-subtropical oceans, pp 261–304

Smith RS, Dubois C, Marotzke J (2006) Global climate and ocean circulation on an aquaplanet Ocean–Atmosphere general circulation model. Journal of Climate 19(18):4719–4737

Trenberth KE, Caron JM (2001) Estimates of meridional atmosphere and ocean heat transports. Journal of Climate 14(16):3433–3443